Journal of Applied Electrochemistry (2005) 35:615–623
DOI 10.1007/s10800-005-2700-x

The function of vinylene carbonate as a thermal additive to electrolyte in lithium batteries

HSIANG-HWAN LEE[1], YUNG-YUN WANG[1], CHI-CHAO WAN[1,*], MO-HUA YANG[2], HUNG-CHUN WU[2] and DENG-TSWEN SHIEH[2]
[1]*Department of Chemical Engineering, National Tsing-Hua University, Hsinchu, Taiwan 300, ROC*
[2]*Materials Reasearch Laboratories of Industrial Technology Reasearch Institute, Chutong, Hsinchu, Taiwan 310, ROC*
*(*author for correspondence, e-mail: ccwan@mx.nthu.edu.tw; fax +886-3-5715408)*

Received 07 December 2004; accepted in revised form 09 February 2005

Key words: additives, high temperature, lithium-ion battery, solid electrolyte interphase, thermal stability, vinylene carbonate

Abstract

The role of vinylene carbonate (VC) as a thermal additive to electrolytes in lithium ion batteries is studied in two aspects: the protection of liquid electrolyte species and the thermal stability of the solid electrolyte interphase (SEI) formed from VC on graphite electrodes at elevated temperatures. The nuclear magnetic resonance (NMR) spectra indicate that VC can not protect $LiPF_6$ salt from thermal decomposition. However, the function of VC on SEI can be observed via impedance and electron spectroscopy for chemical analysis (ESCA). These results clearly show VC-induced SEI comprises polymeric species and is sufficiently stable to resist thermal damage. It has been confirmed that VC can suppress the formation of resistive LiF, and thus reduce the interfacial resistance.

1. Introduction

Safety issues and thermal stability are the major current technological problems for commercial Li-ion batteries. Self-heating of a lithium ion cell via thermal runaway reaction may produce abnormal heat, even smoke and fire. In addition, although lithium ion batteries show excellent performance at room temperature, their usable capacity decreases and internal resistance increases rapidly during cycling and storage at elevated temperatures [1, 2].

Many researchers have focused on the thermal stability of cell materials by means of differential scanning calorimetry (DSC) [3–7] accelerating rate calorimetry (ARC) [8–10], and other analytical methods [11–13]. These results show that the selected electrolyte is critical to the thermal instability of lithium ion batteries [11–13]. $LiPF_6$, the salt most widely used, was found to be one of the important origins for the capacity fade at elevated temperatures because of its insufficient durability against high temperature [11–14]. It tends to thermally decompose into gaseous PF_5 and LiF around 70 °C [13]. The formed PF_5 gas is a very strong Lewis acid and easily reacts with organic solvents or SEI components in Li-ion batteries [1, 11, 12, 14]. Therefore, in recent years, some thermal additives, such as vinylene carbonate (VC) [15, 16] and alkyl borates [16, 17] and other salts [9, 18] with either P or B as a center atom, have been developed to improve thermal stability.

VC as a successful electrolyte additive has been widely used. However, the original purpose of adding it in lithium ion batteries is to overcome graphite exfoliation in PC-based electrolytes [19]. Its high reactivity results from the structure of highly strained cyclic alkyl carbonate and a polymerizable double bond. Previous literature indicates that VC can take part in the formation of the solid electrolyte interphase (SEI), and thus creates an ultra-thin passivating film which inhibits PC co-intercalation or further decomposition and graphite exfoliation [20–23].

Although the contribution of VC to the thermal stability of lithium ion batteries has been established, its actual function in a cell operating or being stored at elevated temperature is not clear yet. According to earlier studies, the thermal instability of $LiPF_6$ is the major factor leading to the fading of usable capacity at high temperature. Hence, in this research, we investigate the changes in $LiPF_6$-based electrolytes by adding or not adding VC at high temperature to clarify if VC stabilizes the electrolytes. Since its effect on the SEI formation and stability may be another factor, we also study the surface compositional change due to addition of VC.

2. Experimental

Ethylene carbonate (EC, battery grade, Merck), diethyl carbonate (DEC, battery grade, Ferro Corp.), vinylene

carbonate (VC, Ferro Corp.), and $LiPF_6$ (Tomiyama) were used as received without further purification. Graphite-based electrodes were made from mesocarbon microbeads (MCMB, Osaka Gas) containing 10 wt% PVDF/HFP (Kureha) binder spread onto a Cu-foil current collector and dried overnight prior to cell assembly. The electrodes contained 10 mg cm^{-2} of active material loading on the current collector.

All experiments were applied to electrolytes with and without VC. Electrolyte preparation and sampling were accomplished in an argon-filled glove box with <0.1 ppm water content, and the water content of these electrolytes were also analyzed by Karl Fischer to be <10 ppm. Various electrolytes were heated at 80 °C for 4 days in vials sealed under Ar atmosphere, and then the solutions were analyzed by Fourier transform infrared spectroscopy (FTIR, Perkin Elmer) and phosphorous-31 nuclear magnetic resonance (NMR, Brucker DMX-600 MHz instrument, H_3PO_4 reference).

For electrochemical testing, coin cells were assembled with a graphite working electrode and a Li foil counter electrode, separated by a PP/PE/PP separator (Celgard, PP: polypropylene, PE: polyethylene) soaked in electrolyte. These cells were pre-cycled five times between 2.0 and 0.0 V vs. Li/Li^+ at room temperature with a current density of 0.3 mA cm^{-2} (about C/10) to form the SEI film for further 80 °C cycling or storage tests. The electrode surfaces were then studied by impedance or electron spectroscopy for chemical analysis (ESCA) methods. All the galvanostatic cycling measurements were carried out by a Maccor series 4000 tester.

An Autolab frequency response analyzer (Eco Chemie, Holland) was used for impedance spectroscopy. The cells with pre-formed SEI on carbon electrodes were fully discharged (lithium atom intercalation into carbon) and carefully dismantled to remove the carbon electrodes in the glove box. Every carbon electrode was cut into two equal pieces and re-assembled to form C/C symmetric coin cells. Then, these cells were stored at 80 °C for 4 days, with their impedance measured daily. Cell impedance was potentiostatically measured by applying an ac bias of 10 mV amplitude, and its frequency was from 50 kHz to 0.01 Hz. All the operations were done in an argon-filled glove box.

Surface change of electrodes before and after 80 °C storage was done with a VG Scientific ESCALAB 250 ESCA spectrometer with monochromatized Al Kα X-ray source (10 K eV). The unstored and stored samples, which were precycled, were taken from opening the Li/C cells in an argon-filled glove box. To prevent the interference of electrolyte species, all samples were washed by DEC and then dried in vacuum.

Cyclic voltammograms were recorded for laboratory type PE cells with lithium counter and reference electrodes and an excess of electrolyte. The electrodes were not closely packed in separator materials but placed in the electrolyte without further support. An Autolab potentiostats (Eco Chemie Inc.) was employed in these measurements.

3. Results and discussions

3.1. *Graphite cycling performance*

The graphite cycling performance is evaluated by the ratio of retentive lithium storage capacity after cycling to the original capacity. Figure 1 shows the capacity retention for electrochemically reversible lithium stored in graphite in EC + DEC (1:1) electrolytes with or without VC at 80 °C. For the system without VC, a dramatic decrease in reversible capacity occurs upon cycling at 80 °C. In the VC-containing case the capacity retention is clearly improved by the addition of VC. Similar results were also reported by Andersson and Edström [1].

3.2. *Thermal reactions of electrolytes*

For a solution with $LiPF_6$ dissolved in organic solvents, the $LiPF_6$ salt is in equilibrium with dissociated ions Li^+ and PF_6^-, (Equation 1). However, partial undissociated $LiPF_6$ may thermally decompose into solid LiF and solvated ions, (Equation 2) [1, 11].

$$LiPF_{6(sol)} \longleftrightarrow Li^+ + PF_6^- \quad (1)$$

$$LiPF_{6(sol)} \xrightarrow{\Delta} LiF_{(s)} + PF_{5(sol)} \quad (2)$$

In a hot environment, PF_5 may react with organic solvent leading to a decrease in PF_5 concentration, so the equilibrium moves toward the right according to Le Chatelier's principle [11]. In this research, two electrolytes containing 1 M $LiPF_6$ dissolved in EC + DEC without and with 2 wt% VC respectively were heated to observe their thermal reactions. The solutions became darkened after being heated for 2 days at 80 °C, and a brown colour and some solid precipitates appeared after 4 days in both systems. These phenomena compared with the original colourless solutions imply that the thermal reaction of $LiPF_6$ occurs whether VC exists or not. So VC does not have any ability to slow down the thermal decomposition of $LiPF_6$. Its function to improve thermal stability must come from other mechanisms.

The phosphorous-31 NMR traces of these two electrolytes before and after 80 °C storage are shown in Figure 2. For the cases before storage (Figure 2a and c), the signals at about −143.7 ppm of chemical shifts relative to H_3PO_4 are typical for the PF_6^- ion [24]. The seven splitting peaks with identical separation are due to the magnetic effects of six coordinated F atoms, which are located in an octahedral structure surrounding the P nucleus. According to first-order rules, when the P nucleus is coupled to six equivalent F nuclei, the P pattern is 7 lines of intensity given by the ratio about 1:6:15:20:15:6:1 [25]. In Figure 2b (the electrolyte w/o VC heated at 80 °C), besides the original ^{31}P signals of PF_6^- new peaks appear at the low-field end of the shift region relative to PF_6^-

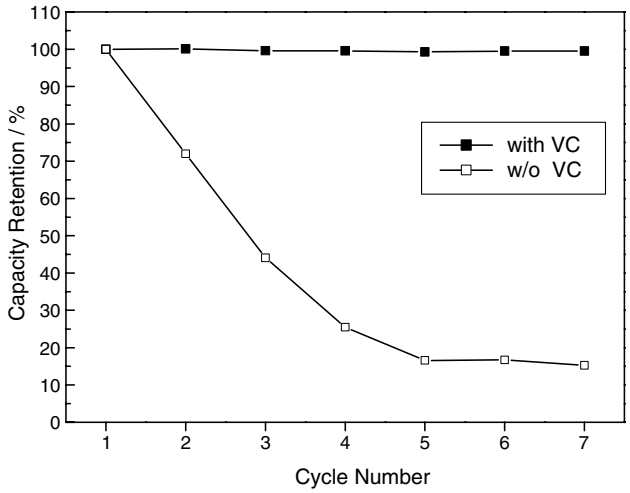

Fig. 1. The cycle performance of Li/C half cells in the electrolytes of $LiPF_6$/EC + DEC with and without VC at 80 °C.

ions. This shows P-containing compounds other than PF_6^- also exist in the electrolyte. Since $LiPF_6$ is the only possible source of P in the initial electrolyte, the other P-containing compounds must come from the thermal decomposition of $LiPF_6$. Furthermore, the new ^{31}P chemical shifts at around −20 ppm are measured downfield from $LiPF_6$, representing lower electronic density around the phosphorous nuclei in the new formed compounds. This is reasonable since the products from thermal decomposition of $LiPF_6$ contain fewer F atoms bonded to the phosphorous center and consequently show lower electronic density around the phosphorous nuclei. Hence, the thermal decomposition of $LiPF_6$ salt may successfully interpret the NMR spectra in Figure 2b.

Interestingly, the same phenomenon also appears in Figure 2d, for the heated electrolyte with VC; the same new peaks appear in the lower field chemical shift region. Consequently, VC can not protect the $LiPF_6$ salt from decomposition at 80 °C. However, the exact forms of the P-containing compounds at around −20 ppm in Figure 2b and d are not yet clear, because the decomposed product in Equation 2, PF_5, is known as a strong Lewis acid and will further react with other chemicals to create new products [11, 12].

Figure 3 shows the results by proton NMR analysis. Based on chemical shifts of the standard spectra [26], four groups of protons (–CH_3 group of DEC, –CH_2 group of EC and DEC, and –CH group of VC) can be labelled in Figure 3. One additional and small singlet labelled as H(4) appears in Figure 3c and e, which exists in cases with and without VC, respectively, after 80 °C storage. According to the gas chromatographic analysis by Sloop et al. [11], the thermal decomposed product, PF_5, may initiate the polymerization of organic solutions. Especially for EC, it will undergo ring opening polymerization to form $[(CH_2CH_2O)_nCOO]_m$ or cap with other components, as in Equations 3 and 4 [11].

$$EC + PF_{5(sol)} \Rightarrow [(CH_2CH_2O)_nCOO]_m \quad (3)$$

$$EC + DMC + PF_{5(sol)} \Rightarrow [-CH_3(O_2COH_2CH_2OCO_2)CH_3-] \quad (4)$$

So based on our NMR spectra, the new singlet is consistent with that reported by Sloop et al. and resembles the peaks of carbonate ester [11]. Consequently, the new proton NMR singlet reveals again that PF_5 will be generated from thermal decomposition of

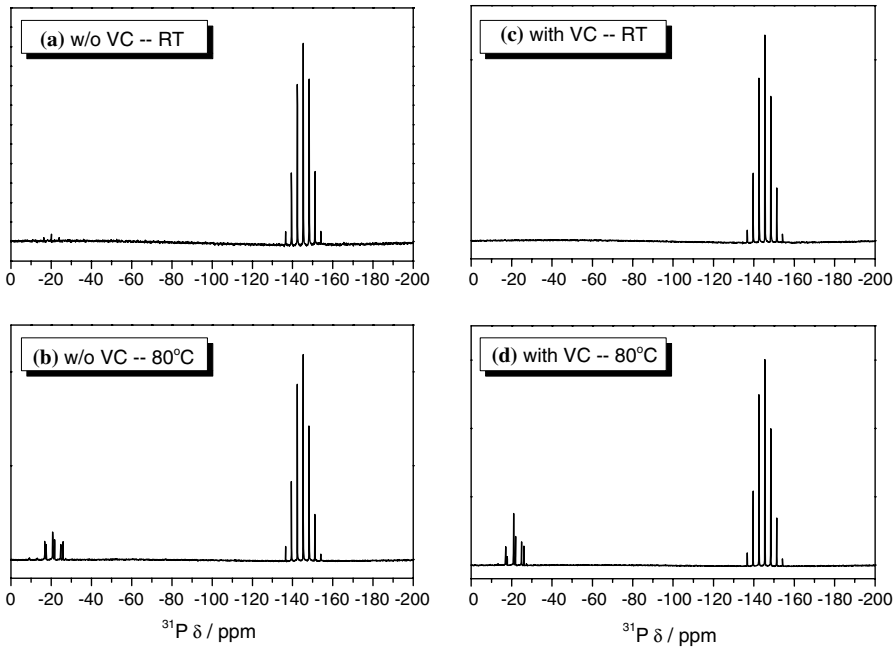

Fig. 2. The phosphorous NMR spectra of electrolytes $LiPF_6$/EC + DEC without VC (a) at room temperature and (b) after storage at 80 °C, and with VC (c) at room temperature and (d) after storage at 80 °C.

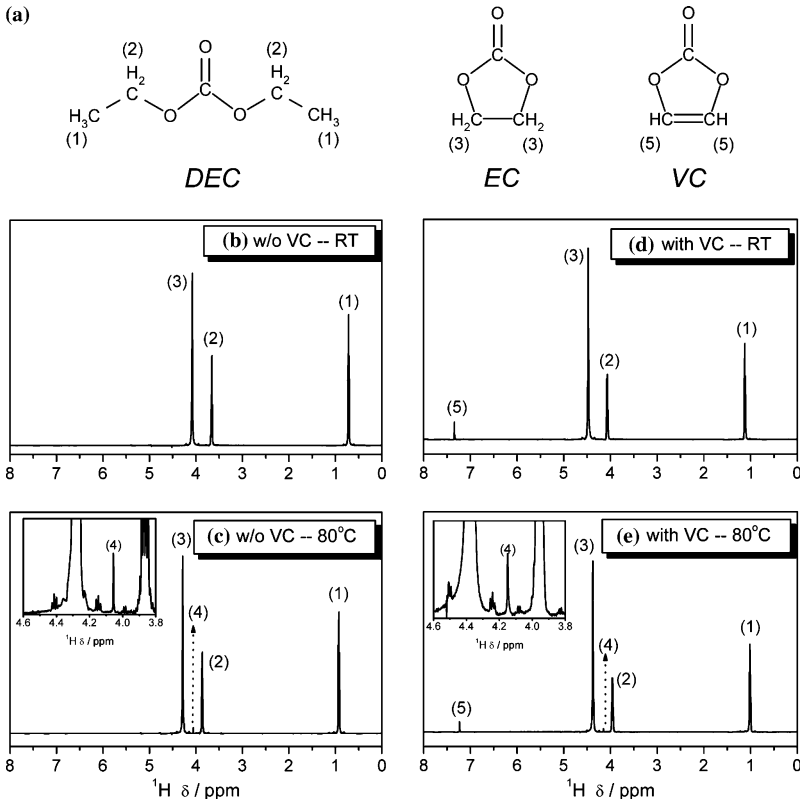

Fig. 3. The proton NMR spectra of electrolytes $LiPF_6$/EC + DEC without and with VC. (a) is the sketch of DEC, EC, and VC structures, and the various protons are labeled. The electrolyte without VC is analyzed (b) at room temperature and (c) after storage at 80 °C; the electrolyte with VC is analyzed (d) at room temperature and (e) after storage at 80 °C. The insets in (c) and (e) are the enlarged view of peak (4).

$LiPF_6$ and induce polymerization whether VC is present or not.

Figure 4 displays the liquid FTIR spectra of the electrolytes without or with VC and at room temperature or at 80 °C. The spectrum for pure VC electrolyte (Figure 4a) is also shown for comparison. The spectra in Figure 4a (pure VC) and d (the electrolyte with VC) show new peaks at 3170 cm^{-1}, which is different from that in Figure 4b (the electrolyte without VC). Hence, this adsorption peak can be attributed to the out-of-plane C–H bending mode of an alkene group (=CH_2) in VC. The absorption peak commonly occurring at 1640 cm^{-1} in Figure 4a, b, and d corresponds to the C=O stretching mode of an alkyl carbonate. Comparing Figure 4b with c, there are no apparent changes of $LiPF_6$/EC + DEC before and after 80 °C storage. Furthermore, the temperature does not seem to affect the IR spectra when VC is added into the same electrolyte (as shown in Figure 4d and e). The polymerization of organic solvents, which is observed in NMR spectra, is not found in IR spectra. That means the major portion of liquid electrolyte still maintains its original structure at 80 °C despite the occurrence of thermal decomposition of $LiPF_6$.

So based on the results of the NMR and FTIR analysis, the electrolytes behave in response to heating in the same way without or with VC. The thermal changes are inevitable in $LiPF_6$/EC + DEC adding VC. $LiPF_6$ salt tends to decompose to produce new compounds, which may induce the polymerization of organic compounds such as the ring opening reaction of EC. So a logical deduction is that the large difference of cycle

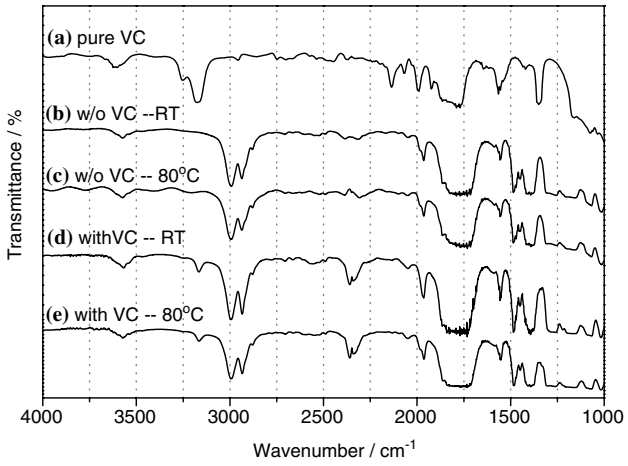

Fig. 4. The FTIR spectra of the liquid electrolytes of 1 M $LiPF_6$ in (a) pure VC, (b) EC + DEC, (c) EC + DEC after 80 °C storage, (d) EC + DEC + 2 wt% VC, (e) EC + DEC + 2 wt% VC after 80 °C storage.

performances at 80 °C shown in Figure 1 must come from other causes, as previously mentioned.

3.3. *Thermal reactions of SEI associated with VC*

The property of SEI is another crucial factor which affects the cycle performance of carbon electrodes. Figure 5 compares the first two voltammetric cycles of graphite electrodes in EC + DEC (1:1) dissolving 1 M $LiPF_6$ without or with 2 wt% VC. Generally speaking, in the first cycle, the oxidative current relates only to lithium deintercalation from graphite; nevertheless, the reductive current includes both lithium intercalation into graphite and the reduction of electrolyte species to form the SEI layer. The SEI formation process is faster than the lithium intercalation, and hence may occur in the higher reductive potential region (>0.3 V vs. Li/Li^+). In Figure 5a (the electrolyte without VC), the reductive current dramatically increases below 0.8 V vs. Li/Li^+, corresponding to the reduction of EC and DEC to form the SEI layer on carbon [27]. However, in the presence of VC (Figure 5b), the apparent rise of reductive current appears at 1.5 V vs. Li/Li^+, which represents the reduction potential of VC [23, 27]. The higher potential of electrolyte with VC than that without VC (Figure 5a) reveals that VC has preferential reduction ability than other solvents. Therefore, if VC exists in the electrolyte, it will react first to form a SEI layer. Previous reports suggest that the SEI formed from the VC-containing electrolyte is capable of inhibiting PC co-intercalation and subsequent graphite exfoliation [19, 23]. Thus VC-induced SEI is more suitable for lithium ion batteries than traditional EC-based electrolytes.

We further utilized impedance methods to observe the interfacial change of pre-cycled graphite electrodes (the SEI is pre-created on electrodes) when stored at 80 °C. Figure 6 shows the Nyquist plots of intercalated electrodes in both electrolytes ($LiPF_6$/EC + DEC without or with VC), which enclose two semicircles and one declining line. As described previously [12, 27], the first semicircle in the high frequency region mainly corresponds to the resistance of the SEI layer on carbon and is a major research area for the thermal stability of the passivated layer. Comparing Figure 6a with b, the trends the impedance change of the first semicircle are apparently different. In Figure 6a (in the absence of VC), the impedance decreases at the beginning and then increases and decreases in an oscillating phenomenon. As discussed earlier [12], the significant shrink of the first semicircle may result from the high attacking ability of PF_5 on SEI. However, the size in the first semicircle increases gradually with prolonged storage in Figure 6b (the electrolyte containing VC). According to the phosphorous NMR spectra (Figure 2d), the thermal decomposition of $LiPF_6$ still proceeds when the electrolyte contains VC. Nevertheless, expanded semicircles in Figure 6b show that the thermal decomposition of $LiPF_6$ leading to the production of PF_5 does not seem to damage the VC-induced SEI. Instead, the SEI grows gradually when stored at high temperature. It is very interesting that VC-induced SEI is not affected by PF_5, but develops to sufficient thickness, exhibiting the desired property of a SEI layer. This finding reveals that the thermal stability of the SEI produced in VC-containing electrolyte is superior to that produced in electrolyte without VC. In other words, the existence of VC has a clear positive impact on the thermal properties of the SEI, leading to the overall improvement in thermal stability of the cell.

To confirm the thermal stability of the VC-induced SEI, we assembled another intercalated C/C symmet-

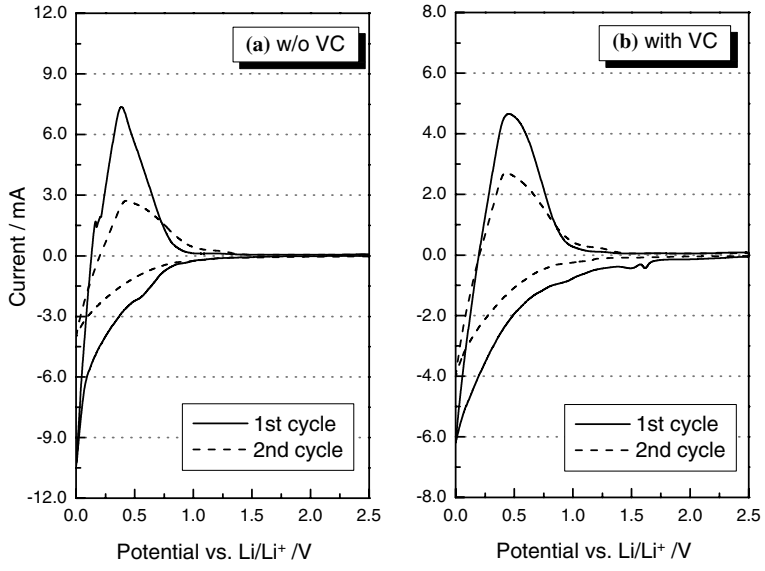

Fig. 5. The first two voltammetric cycles of MCMB graphite electrodes in the electrolytes of (a) 1 M $LiPF_6$/EC + DEC and (b) 1 M $LiPF_6$/EC + DEC + 2 wt% VC with 1 mV s^{-1} scan rate. The solid line marks the first cyclic voltammogram, and the dash line marks the second one in each chart.

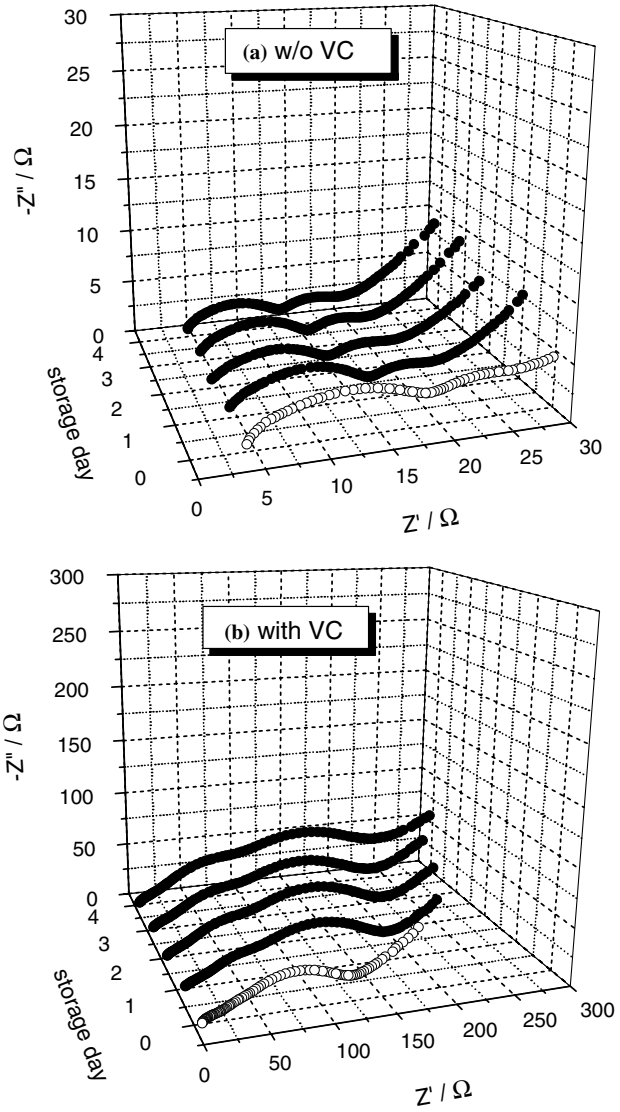

Fig. 6. The time evolution of impedance spectra of a C/C cell with the electrolytes of (a) 1 M $LiPF_6$/EC + DEC and (b) 1 M $LiPF_6$/EC + DEC + 2 wt% VC stored at 80 °C. The carbon electrodes are firstly cycled for 5 times in each electrolyte and then stored in intercalated state.

ric cell with $LiPF_6$/EC + DEC as electrolyte. The cell first underwent 5 formation cycles in $LiPF_6$/EC + DEC + 2 wt% VC electrolyte. The cell impedance at 80 °C is shown in Figure 7. The impedance related to SEI (the first semicircle) gradually increases rather than decreases at the start of storage. This means the SEI layer pre-developed in VC-containing electrolyte is strong enough to resist the destructive reactions induced from heat, such as the electron-attracting reactions of PF_5, even if the SEI layer later resides in an environment without VC. Hence, Figure 7 proves again that VC has a dominant influence on SEI, and its existence greatly benefits the thermal stability of SEI in lithium ion batteries.

In order to verify why the VC-induced SEI is so excellent, ESCA was used to probe the species present in the SEI on graphite electrodes in the presence or absence of VC. Figure 8 displays the ESCA spectra of

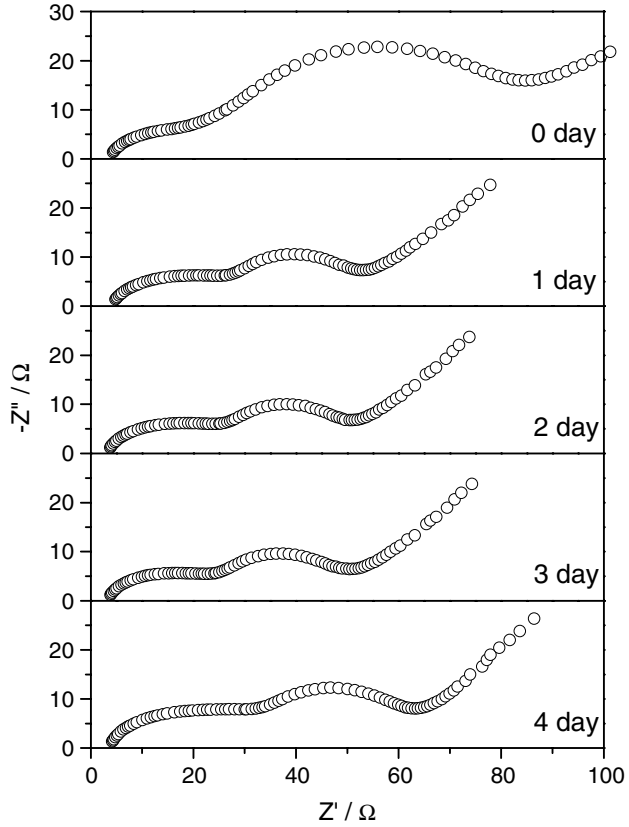

Fig. 7. The time evolution of impedance spectra of a C/C cell with PP/PE/PP in 1 M $LiPF_6$/EC + DEC (v/v = 1:1) stored at 80 °C. The carbon electrode is firstly cycled for 5 times in 1 M $LiPF_6$/EC + DEC + 2 wt% VC to create the SEI film and stored in intercalated state.

F, Li, C, and O for the graphite electrodes cycled in these two electrolytes. The possible species are also designated in every spectrum [1, 27–29]. The spectra for the SEI produced in electrolytes without VC (Figure 8a) and with VC (Fig. 8b) are very similar except the F1s spectrum. In general, the broad peak ranging between 52 and 58 eV in the Li1s spectrum is superimposed by Li–O bonding of lithium carbonate, alkoxide, or hydroxide (55 eV) and LiF (56 eV) [1, 28]. The O1s spectrum includes a broad superposition of a peak around 532 eV, which is attributable to carbonate including Li_2CO_3 and $ROCO_2Li$. For the C1s spectrum, three main peaks are characterized at around 285, 287, and 290 eV. According to Schechter and Aurbach [28], Li_2CO_3 shows a peak at 290 eV or higher due to charging. The broad superposition of a peaks at 287–288 eV is assigned to the ether carbon of various $ROCO_2Li$ species. In the EC-based electrolyte, $(CH_2OCO_2Li)_2$, the major reduction product of EC, is usually the most dominant one (like C1s spectrum in Figure 8a) [12, 28, 29]. The peak around 285 eV corresponds to the hydrocarbons of lithium alkyl–carbonate, especially the polymers in SEI layers. The 285 eV peak of the C1s spectrum in Figure 8b (the VC-containing electrolyte) is more pronounced than other peaks. Compared to Figure 8a (without VC case) this peak, assigned to the polymers seems to

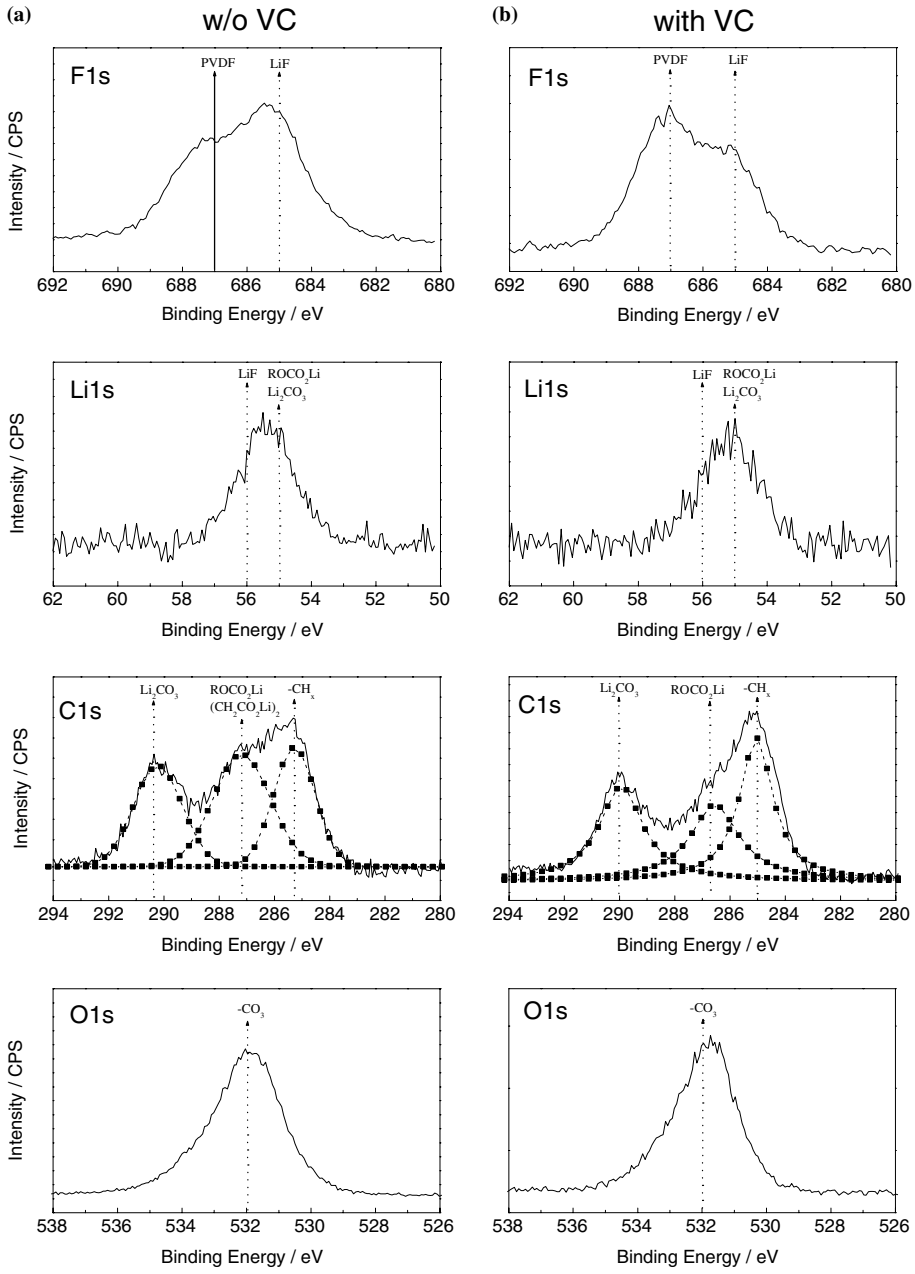

Fig. 8. F1s, Li1s, C1s, and O1s ESCA spectra of graphite electrodes cycled in 1 M $LiPF_6$/EC + DEC (v/v = 1:1) (a) without VC and (b) with 2 wt% VC.

dominate the spectrum over the other peaks. In the cyclic voltammograms of Figure 5, VC is more electrochemically active than the other solvents like EC or DEC, and the reduction products from VC hence dominate over other species when the electrolyte contains it. These results indicate that the major component of the VC-induced SEI is attributable to the reduction of VC to polymeric-type species, which is different from the conventional SEI species, $(CH_2OCO_2Li)_2$, in EC-based electrolytes. Some papers [21, 27, 30–36] suggest that VC and its reduction products easily polymerize via their carbonate group

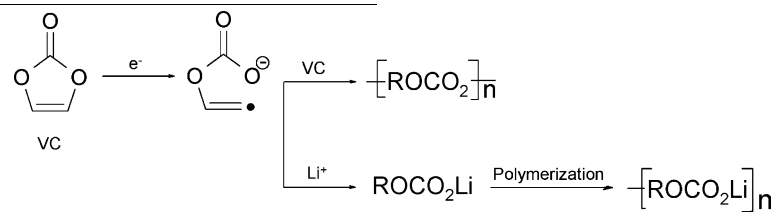

(5)

or double bond to form polycarbonate (like Equation 5), and match our ESCA results.

The most noteworthy thing is that the F1s spectrum related to the electrolyte without VC (Figure 8a) shows a pronounced LiF peak at 685 eV, but that related to the electrolyte with VC (Figure 8b) has its main peak at 687 eV, which is assigned to the PVdF binder [27]. This clear difference reveals that large amounts of LiF are formed in $LiPF_6$/EC + DEC via electrochemical cycles, but the addition of VC to the electrolyte can suppress its production. Several possible LiF formation reactions by charge transfer or trace amounts of water have been described [1, 28–29].

$$PF_6^- + 2e^- + 3Li^+ \rightarrow 3LiF + PF_3 \quad (6)$$

$$LiPF_{6(sol)} + H_2O \rightarrow LiF + 2HF + POF_3 \quad (7)$$

$$PF_5 + 2xe^- + 2xLi^+ \rightarrow xLiF + Li_xPF_{5-x} \quad (8)$$

$$POF_3 + 2xe^- + 2xLiF + Li_xPF_{3-x}O \quad (9)$$

We postulate that VC is prone to attract electrons or react with water, so that the above reactions to form LiF are inhibited. LiF also plays an important role in cell performance at high temperature because it is insulating and a large amount of LiF formed on the graphite electrodes will gradually block the electrodes. On the contrary, the addition of VC can inhibit the formation of LiF, and thus successfully promotes the cycling, especially at elevated temperatures. Similar results were also found by Aurbach et al. [27].

Consequently, the presence of VC has two impacts on the formation of SEI. One is to change the major component of SEI. VC could predominate the reduction process of electrolytes, and hence produces the polymeric species instead of $(CH_2OCO_2Li)_2$, the reduction product of EC. The other is to reduce the production of LiF.

Similar C1s ESCA data for both samples stored at 80 °C for 4 days are displayed in Figure 9. The corresponding spectra before 80 °C storage are also presented as the dashed line for comparison. There are some changes before and after high temperature storage in the Figure 9a (the electrolyte without VC). The carbonate peak (290 eV) apparently dominates in the storage case. When compared to the unstored sample, carbonate compounds are substantially produced after storage at high temperature. According to Andersson and Edström's suggestions [1], Li-alkyl-carbonate which is the major component of SEI layer due to the reduction of EC would thermally decompose to the stable Li_2CO_3. Additionally, our previous research suggests PF_5, the thermal decomposed product of $LiPF_6$, is the major factor to harm the SEI by means of electron withdrawing reactions [12]. The related reaction is like Equation 10.

$$(CH_2OCO_2Li)_2 \xrightarrow{\Delta, PF_5} Li_2CO_3 + \text{gases} \quad (10)$$

This may account for the large increase in intensity of the 290 eV peak, and also the decrease in the SEI impedance in Figure 6a.

However, the spectrum of the VC-containing case (Figure 9b) retains its pattern after 80 °C storage. This similarity indicates the quite stable property of VC-induced SEI (the polymeric species) even when it is baked at 80 °C. The semicircle gradually grows indicating instead of thermally decomposition. From the phosphorous NMR spectra in Figure 2, the thermal decomposition of $LiPF_6$ appears in both cases. However, this thermally induced damage does not occur in VC-induced SEI. This means that the polymer species formed from the VC-containing electrolyte are much more stable than those from the electrolyte without VC. This kind of polymeric SEI is stable enough to prevent the thermal decomposition or PF_5 attacking (Equation 10). Hence, the ESCA data provide further proof that, if VC is present in the electrolyte, it dominates the formation of SEI and benefits thermal stability.

4. Conclusion

The reason why VC, when used in lithium ion batteries, promotes thermal stability has been clarified. The NMR

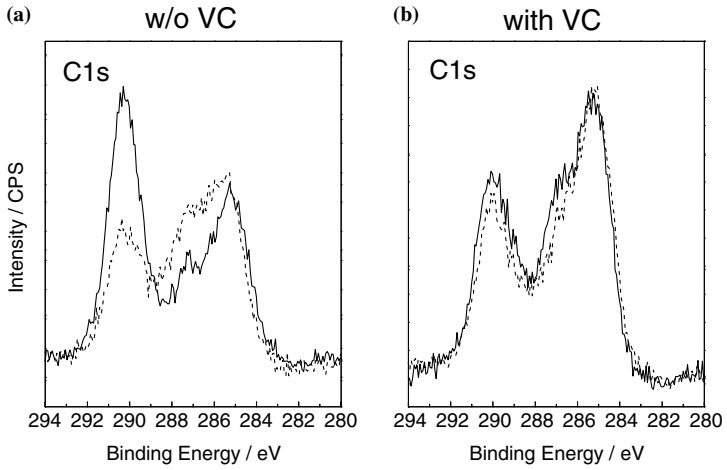

Fig. 9. The C1s ESCA spectra of graphite electrodes taken from precycled cells and then stored at 80 °C for 4 days (solid line) in 1 M $LiPF_6$/EC + DEC (v/v = 1:1) (a) without VC and (b) with 2 wt% VC. The spectra of unstored samples (dash line) are also presented for comparison.

and FTIR spectral studies indicate the thermal decomposition of $LiPF_6$ salt is unavoidable despite the addition of VC. The major cause comes from its protective effect on the SEI formed on the graphite electrode.

Two major advantages can be realized with the addition of VC in $LiPF_6$/ EC + DEC electrolyte. The SEI induced from VC is quite stable especially at elevated temperatures. We attribute the thermal stability of SEI to the ability of VC to form polyvinylene carbonate because VC is reduced predominantly on graphite electrodes in $LiPF_6$/EC + DEC + 2 wt% VC electrolyte. This polymeric species are capable of resisting the attack of PF_5 or other thermal reactions, and by provide better passivation than surface films comprising $(CH_2OCO_2Li)_2$, which is the major SEI component in $LiPF_6$/EC + DEC without VC. The other advantage of using VC is that it can suppress the production of LiF during prolonged cycling and thus reduce the surface resistance of the graphite electrode. Consequently, a stable SEI layer with few resistive products formed on a graphite electrode leads to a cell having improved thermal cycling performance.

Acknowledgements

The technical support of Materials Reasearch Laboratories of Industrial Technology Reasearch Institute (Taiwan) is acknowledged. The ESCA analysis done by Ms. Hsiang-Ping Wen of the Instrumentation Center in National Taiwan University is especially appreciated.

References

1. A.M. Andersson and K. Edström, *J. Electrochem. Soc.* **148** (2001) A1100.
2. A.M. Andersson, K. Edström, N. Rao and A. Wendsjö, *J. Power Sources* **81–82** (1999) 286.
3. J.I. Yamaki, H. Takatsuji, T. Kawamura and M. Egashira, *Solid State Ionics* **148** (2002) 241.
4. U.V. Sacken, E. Nodwell, A. Sundher and J.R. Dahn, *J. Power Sources* **54** (1995) 240.
5. F. Joho, P. Novák and M.E. Spahr, *J. Electrochem. Soc.* **149** (2002) A1020.
6. A.D. Pasquier, F. Disma, T. Bowmer, A.S. Gozdz, G. Amatucci and J.M. Tarascon, *J. Electrochem. Soc.* **145** (1998) 472.
7. N. Katayama, T. Kawamura, Y. Baba and J.I. Yamaki, *J. Power Sources* **109** (2002) 321.
8. M.N. Richard and J.R. Dahn, *J. Electrochem. Soc.* **146** (1999) 2068.
9. J. Jiang and J.R. Dahn, *Electrochem. Commun.* **6** (2004) 39.
10. D.D. MacNeil, D. Larcher and J.R. Dahn, *J. Elecrochem. Soc.* **146** (1999) 3596.
11. S.E. Sloop, J.K. Pugh, S. Wang, J.B. Kerr and K. Kinoshita, *Electrochem. Solid-State Lett.* **4** (2001) A42.
12. H.H. Lee, C.C. Wan and Y.Y. Wang, *J. Elecrochem. Soc.* **151** (2004) A542.
13. X. Zhang, P.N. Ross Jr., R. Kostecki, F. Kong, S. Sloop, J.B. Kerr, K. Striebel, E.J. Cairns and F. McLarnon, *J. Elecrochem. Soc.* **148** (2001) A463.
14. K. Araki and N. Sato, *J. Power Sources* **124** (2003) 124.
15. R. Oesten, U. Heider and M. Schmidt, *Solid State Ionics* **148** (2002) 391.
16. M. Contestabile, M. Morselli, R. Paraventi and R.J. Neat, *J. Power Sources* **119–121** (2003) 943.
17. S.S. Zhang, K. Xu and T.R. Jow, *Electrochem. Solid-State Lett.* **5** (2002) A206.
18. J. Jiang and J.R. Dahn, *Electrochem. Solid-State Lett.* **6** (2003) A180.
19. B. Simon and J.P. Boeuve US Patent No. 5,626,981 (1997).
20. O. Matsuoka, A. Hiwara, T. Omi, M. Toriida, T. Hayashi, C. Tanaka, Y. Saito, T. Ishida, H. Tan, S.S. Ono and S. Yamamoto, *J. Power Sources* **108** (2002) 128.
21. K.C. Möller, H.J. Santner, W. Kern, S. Yamaguchi, J.O. Besenhard and M. Winter, *J. Power Sources* **119–121** (2003) 561.
22. S.K. Jeong, M. Inaba, R. Mogi, Y. Iriyama, T. Abe and Z. Ogumi, *Langmuir* **17** (2001) 8281.
23. X. Zhang, R. Kostecki, T.J. Richardson, J.K. Pugh and P.N. Ross Jr., *J. Elecrochem. Soc.* **148** (2001) A1341.
24. E. Fluck and G. Heckmann, in J.G. Verkade and K.D. Quin (Eds), 'Ch. 2 in Phosphorous-31 NMR Spectroscopy in Stereochemical Analysis – Organic Compounds and Metal Complexes', (Wiley-VCH, Weinheim, 1987).
25. R.J. Abraham, J. Fisher and L. Loftus, *Introduction to NMR spectroscopy*, 2nd ed., (John Wiley & Sons, Essex, 1987), pp. 1.
26. Spectral Data Base System for Organics Compounds (SDBS), www.aist.go.jp/ RIDDB/SDBS/menu-e.html.
27. D. Aurbach, K. Gamolsky, B. Markovsky, Y. Gofer, M. Schmidt and U. Heider, *Eelectrochim. Acta* **47** (2002) 1423.
28. A. Schechter and D. Aurbach, *Langmuir* **15** (1999) 3334.
29. D. Aurbach, I. Weissman and A. Schechter, *Langmuir* **12** (1996) 3991.
30. H. Ota, K. Shima, M. Ue and J. Yamaki, *Electrochim. Acta* **49** (2004) 565.
31. Y. Wang and P.B. Balbuena, *J. Phys. Chem. B* **106** (2002) 4486.
32. L. Ding, Y. Li, Y. Li, Y. Liang and J. Huang, *European Polymer J.* **37** (2001) 2453.
33. H. Ota, Y. Sakata, Y. Otake, K. Shima, M. Ue and J. Yamaki, *J. Elecrochem. Soc.* **151** (2004) A1778.
34. H. Ota, Y. Sakata, A. Inoue and S. Yamahuchi, *J. Elecrochem. Soc.* **151** (2004) A1659.
35. D. Aurbach, J.S. Gnanaraj, W. Geissler and M. Schmidt, *J. Elecrochem. Soc.* **151** (2004) A23.
36. M. Herstedt, A.M. Andersson, H. Rensmo, H. Sigbahn and K. Edströem, *Electrochim. Acta* **49** (2004) 4939.